



<https://doi.org/10.31217/p.39.2.8>

# Developing an AIS Big Data-Driven Framework for Ship Emission Monitoring in Ports

Andi Wibisono, Achmad Riadi\*, Muhammad Aqil Taqiyyuddin, Muhammad Arif Budiyo, Dimas Angga Fakhri Muzhoffar

Departemen Teknik Mesin, Fakultas Teknik, Universitas Indonesia, Depok, Jawa Barat 16424, Indonesia, e-mail: andiwibisono101300@gmail.com; achmadriadi@ui.ac.id; muhammad.aqil01@ui.ac.id; arif@eng.ui.ac.id; dimas.anggafm@ui.ac.id

\* Corresponding author

## ARTICLE INFO

### Original scientific paper

Received 17 March 2025

Accepted 13 May 2025

### Key words:

Ship emission

Emission monitoring

Tanjung Priok Port

Automatic Identification System (AIS)

Big data

Maritime transportation

## ABSTRACT

The rapid expansion of maritime transportation has significantly impacted air quality due to increased ship emissions. This study aims to develop a ship emission monitoring system utilizing Automatic Identification System (AIS) big data, with Tanjung Priok Port in Indonesia (ID TPP) as the case study. The system is designed to monitor and analyze ship emissions based on historical AIS data, providing actionable insights to mitigate environmental impacts. By integrating various data processing techniques, including data preprocessing, database development, sailing time and speed calculation, and emission estimation, this research provides a comprehensive framework for a ship emission monitoring system. The system can be implemented in ports through the development of an interactive web-based dashboard, enhancing the decision-making capabilities of port authorities and other stakeholders. The results demonstrate the system's potential for effectively monitoring emissions and promoting sustainable maritime operations.

## 1 Introduction

Over the past few decades, the substantial growth of maritime transportation has exerted a significant impact on air quality. Approximately 90% of global traffic is transported by sea, contributing significantly to environmental pollution. Studies show that ships emit various pollutants into the atmosphere, including  $\text{NO}_x$ ,  $\text{CO}_2$ , volatile organic compounds,  $\text{SO}_x$ , and particulate matter. Ships account for 2.2% of global  $\text{CO}_2$  emissions and a large percentage of  $\text{NO}_x$  and  $\text{SO}_2$  emissions. The shipping industry contributes approximately 1.056 billion tons of  $\text{CO}_2$  annually, accounting for 2.9% of global greenhouse gas emissions. This amount is projected to rise substantially over the next 10 to 40 years, driven by the anticipated growth in international trade activities [1], [2].

These pollutants contribute to adverse health effects, environmental degradation, and reduced air quality in densely populated coastal areas [3], [4], [5], [6],

[7]. Previous studies have shown that shipping emissions directly impact around 230 million people globally. In 2016, East Asia experienced over 24,000 premature deaths annually attributed to these emissions [8]. Without intervention, shipping-related pollution could increase by 150 to 250% globally by 2050, posing greater health risks to the public [9], [10]. About 70% of ship emissions occur within 400 km of the coast, significantly impacting air quality in coastal and urban areas. High ship traffic in ports degrades air quality, highlighting the need for detailed ship emission inventories and continuous monitoring to support effective management strategies [11].

Many researchers have used the Ship Traffic Emission Assessment Model (STEAM) with Automatic Identification System (AIS) big data to estimate ship emissions in ports. AIS big data refers to the large-scale collection, processing, and analysis of AIS signals transmitted by ships worldwide. AIS is a maritime communication sys-

tem used for vessel tracking and collision avoidance, and its data contains valuable information about ship movements. The activity-based method calculates emissions by identifying ship activities and their respective emission factors, offering detailed statistical analysis of emission sources. For example, research demonstrated that STEAM could accurately estimate emissions from maritime traffic by integrating AIS data with ship engine characteristics and fuel consumption rates [12]. More recently, research highlighted the importance of real-time AIS data processing for monitoring emissions in dynamic port environments, showing that delays in data handling could lead to significant underestimations of short-term emission spikes [13]. However, real-time AIS data processing remains crucial for timely monitoring and management of pollution.

AIS enhances navigation safety and communication among ships by providing real-time static and dynamic data. Despite its benefits, processing AIS data requires significant effort to ensure accuracy and efficiency in real-time emission assessment. For instance, some studies emphasized that AIS-based emission models must account for data gaps, errors, and inconsistencies to produce reliable estimations. Meanwhile, a research demonstrated that real-time AIS data processing could significantly improve the temporal resolution of ship emission monitoring, allowing for more responsive environmental management [14]. These findings highlight the need for robust data processing techniques to maximize the potential of AIS in emission assessments.

Although there has been extensive research on ship emission monitoring systems, this study differs by focusing on Tanjung Priok Port in Indonesia (ID TPP). As a major hub in the Southeast Asia region, this port is crucial for the national economy and significantly impacts environmental quality. This research aims to develop a real-time ship emission monitoring system using AIS data by employing Python programming and the Django framework. Django serves as the backbone of the web-based system, handling data processing, database management, and real-time visualization through an interactive dashboard. By integrating Django with a MySQL database and AIS data processing scripts, the system enables automated emission calculations and provides critical data for policymakers to effectively mitigate environmental impacts. This study also addresses challenges such as mapping zone accuracy, data collection periods, and data visualization.

## 2 Materials and Methods

### 2.1 Identification of Ship Trajectories

The process of identifying ship trajectories is conducted to determine the direction of ship movement when entering the Port area. This identification process

uses AIS data variables that have undergone pre-processing. Maritime Mobile Service Identity (MMSI) and International Maritime Organization (IMO) data are used to identify each ship. MMSI is used because it has a unique identification system for each ship and is automatically registered in the AIS data (while the IMO number must be manually entered by the crew, allowing for potential errors). Longitude and latitude data are then used to determine the coordinates of the ship on the map. Latitude and longitude are measured based on Earth's coordinate parameters, making them accurate indicators of the ship's position. The final data used is the timestamp data, which indicates the time the AIS data was collected.

Using a combination of these AIS data, the ship's trajectory or path can be constructed based on the collected timestamps. This trajectory can be used to identify the ship's position and how long it remained in that position. Additionally, the ship's trajectory can be calculated to determine its speed.

As shown in Figure 1, the sampling period is structured over designated time intervals, enabling the acquisition of AIS data streams in continuous data blocks. Within each block, ship trajectories are extracted initially for various vessels. Given the essential role of Maritime Mobile Service Identity (MMSI) in uniquely identifying individual ships, AIS messages containing the same MMSI within a data block can be consolidated.

### 2.2 Ship Traffic Emission Assessment Model (STEAM)

The Ship Traffic Emission Assessment Model (STEAM) was developed by Jalkanen [12] as a framework to measure and analyze emissions from maritime traffic. By collecting data on ship movements, fuel consumption, and engine characteristics, STEAM provides accurate emission estimates. Considering various pollutants such as CO<sub>2</sub>, NO<sub>x</sub>, SO<sub>x</sub>, and particulate matter (PM), The STEAM model facilitates a deeper understanding of the environmental impacts associated with maritime activities. STEAM is a crucial tool for researchers and policymakers to formulate emission mitigation strategies in the shipping sector.

STEAM is an estimation model that assesses emissions based on input data such as ship activity, engine specifications, and emission factors. This method has been successfully applied in Various studies that provided insights that support global decision-making processes [15], [16], [17]. Figure 2 presents the STEAM model framework, which relies on data from multiple sources. These include Lloyd's List Intelligence for information on the power and tonnage of heavy equipment, as well as Automatic Identification System (AIS) data for tracking ship types, sailing durations, and speeds. Additionally, empirical values from prior research are utilized for correction factors and emission coefficients.

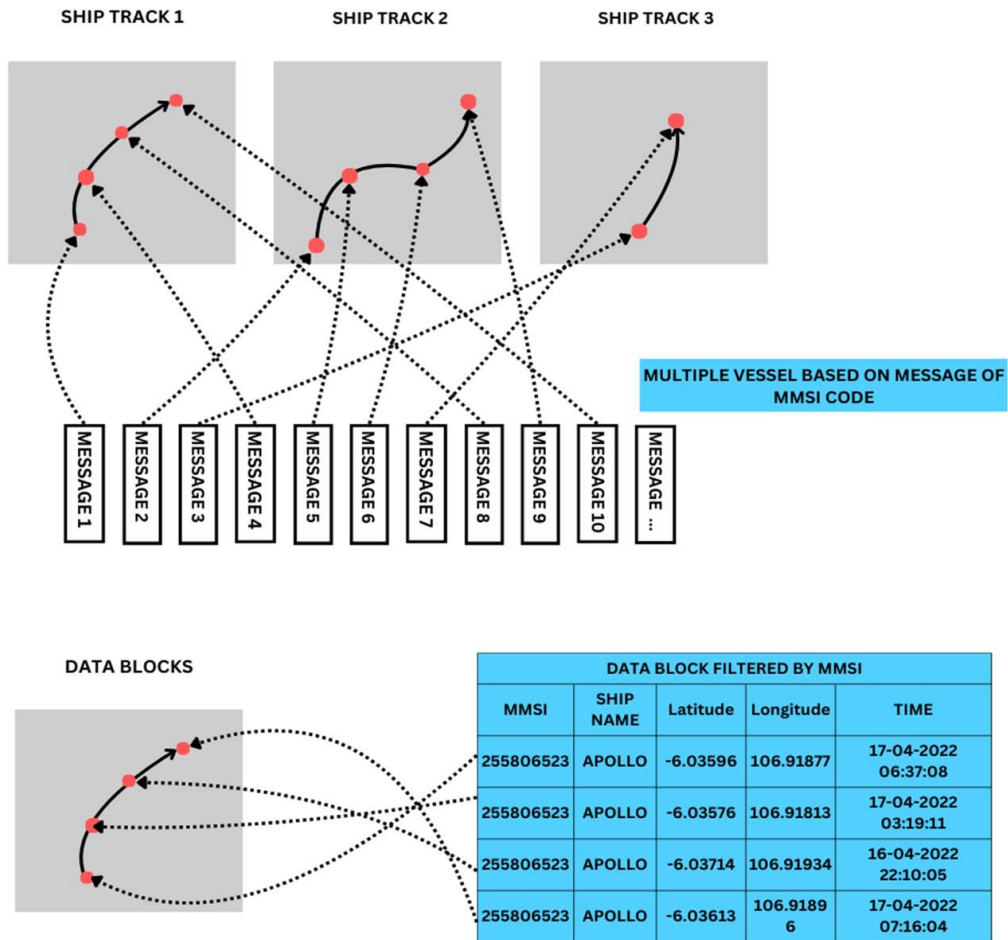


Figure 1 AIS Data Stream Splitting

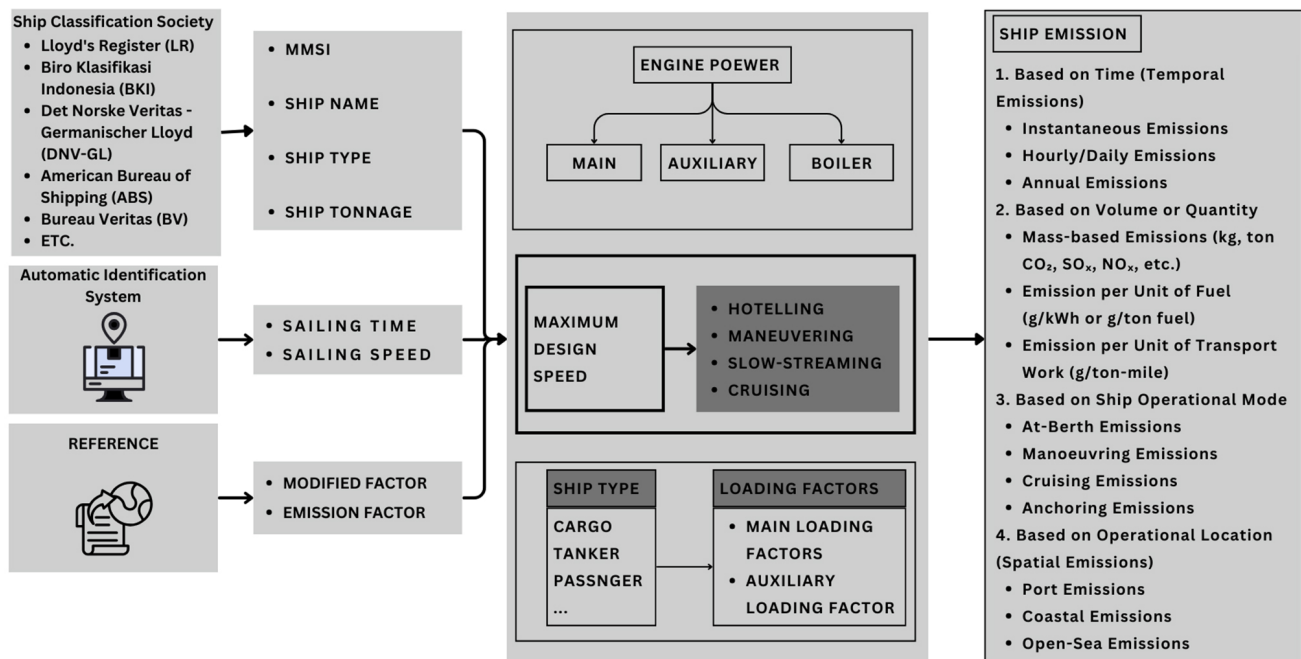


Figure 2 STEAM Method Flow

The diagram in Figure 2 highlights key components of the STEAM method, including inputs like the ship's main engine power, auxiliary engine power, and tonnage, which influence the calculation of maximum design speed. These inputs are critical for determining emission factors, which are adjusted using data from Lloyd's databases, AIS data, and reference values.

Studies such as [18] have emphasized the importance of integrating data sources to ensure accurate emission assessments. Different types of ships have varying power levels, directly affecting their emissions. Generally, ships utilize three primary power sources: main engines, auxiliary engines, and boilers [19]. Emissions from these engines can be estimated using specific equations 1 – 3 outlined in the literature [16], [20].

Main Engine:

$$E_{a,i} = (P_a \times L_a \times T_a \times E_{Fa}) / 10^3 \quad (1)$$

Auxiliary Engine:

$$E_{b,i} = (P_b \times L_b \times T_b \times E_{Fb}) / 10^3 \quad (2)$$

Boiler:

$$E_{c,i} = (P_c \times E_{Fc} \times T_c) / 10^3 \quad (3)$$

The notation description of the formula is explained as presented in Table 1.

**Table 1** Notation description of the emissions from different engines equation

| Notation   | Description   |
|------------|---|
| $i$        | The type of pollutant emitted, including CO, CO <sub>2</sub> , NMVOC, NO <sub>x</sub> , PM <sub>2.5</sub> , SO <sub>2</sub>   |
| $E_{a,i}$  | The emission of the ship's main engine for different pollutants (units: Kg)   |
| $E_{b,i}$  | The emission of the ship's auxiliary engine for different pollutants (units: Kg)  |
| $E_{c,i}$  | The emission of the ship's boiler for different pollutants (units: tone)  |
| $p_a$      | Ship's power for Main Engine (units: kW)  |
| $p_b$      | Ship's power for Auxiliary Engine (units: kW)   |
| $p_c$      | Ship's power for Boiler Engine (units: kW)  |
| $L_a, L_b$ | The load factor for the main and auxiliary engines, where the value is obtained from the actual speed and the ship's maximum speed: $L = V_{act} / V_{max}$ ; $V_{act}$ indicates the actual speed; $V_{max}$ indicates the maximum speed |
| $EF_a$     | The emission factor of the main engine (units: g/kWh)   |
| $EF_b$     | The emission factor of the auxiliary engine (units: g/kWh)  |
| $T_a$      | Operating time of the main engine (unit: hours)   |
| $T_b$      | Operating time of the auxiliary engine (unit: hours)  |
| $T_c$      | Operating time of the boiler (unit: hours)  |

Table 1 presents the notation used in ship emission calculations, detailing various pollutants such as CO, CO<sub>2</sub>, NOX, and SO<sub>2</sub>. It defines emissions from different sources, including the main engine, auxiliary engine, and boiler, along with their respective power outputs. The table also introduces load factors for the main and auxiliary engines, calculated based on the ratio of actual speed to maximum speed. Furthermore, it includes emission factors specific to each engine type, which are essential for accurately assessing and quantifying ship emissions.

### 2.3 Load Factor

The load factor for the main engine (ME) is calculated using the Propeller Law, as defined by the Port of Long Beach [21], and is expressed by the following equation 4.

$$LF = \left( \frac{AS}{MS} \right)^3 \quad (4)$$

In this equation, LF represents the load factor of the main engine, AS is the actual operating speed (knots), and MS denotes the maximum speed (knots). The maximum speed data for each ship is obtained from sources such as Lloyd's database, the CCS database, or prior research and surveys, while the actual speed is calculated by dividing the distance traveled between two AIS-reported positions by the time interval between them.

Within the STEAM model, the emission factor varies based on changes in the load factor of the main engine [22], [24], [25]. Specifically, when the load factor is below 20%, a correction factor is applied to the emission factor, as shown in Table 2. For auxiliary engines, the load factor is based on the ship's type and activity, as shown in Table 3.

### 2.4 Ship Emission

Ship emissions refer to the release of various pollutants into the air resulting from the operational activities of sea vessels. These pollutants are produced during the fuel combustion process in ship engines. Types of ship emissions involve harmful gases and particles that can affect air quality around water areas and significantly contribute to environmental impact.

The primary types of ship emissions are categorized and shown in Table 4. The emission factors used in this study are derived from previous ship emission inventories [16].

**Table 2** Emission Correction Factor for Main Engine at Low Load [22]

| Load | SO <sub>2</sub> | NO <sub>x</sub> | PM    | NMVOC | CO    | CO <sub>2</sub> |
|------|-----------------|-----------------|-------|-------|-------|-----------------|
| 0.01 | 1.00            | 11.47           | 19.17 | 59.28 | 19.32 | 1.00            |
| 0.02 | 1.00            | 4.63            | 7.29  | 21.18 | 9.68  | 1.00            |
| 0.03 | 1.00            | 2.92            | 4.33  | 11.68 | 6.46  | 1.00            |
| 0.04 | 1.00            | 2.21            | 3.09  | 7.71  | 4.86  | 1.00            |
| 0.05 | 1.00            | 1.83            | 2.44  | 5.61  | 3.89  | 1.00            |
| 0.06 | 1.00            | 1.60            | 2.04  | 4.35  | 3.25  | 1.00            |
| 0.07 | 1.00            | 1.45            | 1.79  | 3.52  | 2.79  | 1.00            |
| 0.08 | 1.00            | 1.35            | 1.61  | 2.95  | 2.45  | 1.00            |
| 0.09 | 1.00            | 1.27            | 1.48  | 2.52  | 2.18  | 1.00            |
| 0.10 | 1.00            | 1.22            | 1.38  | 2.20  | 1.96  | 1.00            |
| 0.11 | 1.00            | 1.17            | 1.30  | 1.96  | 1.79  | 1.00            |
| 0.12 | 1.00            | 1.14            | 1.24  | 1.76  | 1.64  | 1.00            |
| 0.13 | 1.00            | 1.11            | 1.19  | 1.60  | 1.52  | 1.00            |
| 0.14 | 1.00            | 1.08            | 1.15  | 1.47  | 1.41  | 1.00            |
| 0.15 | 1.00            | 1.06            | 1.11  | 1.36  | 1.32  | 1.00            |
| 0.16 | 1.00            | 1.05            | 1.08  | 1.26  | 1.24  | 1.00            |
| 0.17 | 1.00            | 1.03            | 1.06  | 1.18  | 1.37  | 1.00            |
| 0.18 | 1.00            | 1.02            | 1.04  | 1.11  | 1.11  | 1.00            |
| 0.19 | 1.00            | 1.01            | 1.02  | 1.05  | 1.05  | 1.00            |
| 0.20 | 1.00            | 1.00            | 1.00  | 1.00  | 1.00  | 1.00            |

**Table 3** Auxiliary Engine Load Factor Assumptions [23]

| Ship Type     | Sailing | Manoeuvring | Mooring |
|---------------|---------|-------------|---------|
| Auto carrier  | 0.13    | 0.67        | 0.24    |
| Bulk carrier  | 0.17    | 0.45        | 0.22    |
| General cargo | 0.17    | 0.45        | 0.22    |
| Tanker        | 0.13    | 0.45        | 0.67    |
| Container     | 0.13    | 0.5         | 0.17    |
| Reefer        | 0.20    | 0.67        | 0.34    |
| Passenger     | 0.80    | 0.8         | 0.64    |
| Ro-ro         | 0.15    | 0.45        | 0.3     |
| Rest          | 0.17    | 0.45        | 0.22    |

**Table 4** Ship Emission Description

| Pollutant   | Description  | Impact   |
|---|--|--|
| NO <sub>x</sub> (Nitrogen Oxides)                         | Irritant gases, including NO and NO <sub>2</sub> , are produced from high-temperature fuel combustion. | Causes respiratory issues, acid rain, and smog formation.                      |
| PM <sub>10</sub> , PM <sub>2.5</sub> (Particulate Matter) | Fine particles with diameters ≤10 µm or ≤2.5 µm. Emitted from fuel combustion and engine wear.         | It can penetrate human lungs, causing respiratory and cardiovascular diseases. |
| CO (Carbon Monoxide)                                      | Produced from incomplete combustion of fossil fuels.   | Harmful to human health; reduces oxygen delivery in the bloodstream.           |
| SO <sub>x</sub> (Sulfur Oxides)                           | Formed from burning sulfur-containing fuels, primarily HFO (Heavy Fuel Oil).                           | Causes respiratory and cardiovascular issues; contributes to acid rain.        |
| NMVOC (Non-Methane Volatile Organic Compounds)            | Organic compounds emitted from fuel evaporation and combustion.  | Contributes to ground-level ozone and secondary pollutant formation.           |
| CO <sub>2</sub> (Carbon Dioxide)                          | The main greenhouse gas emitted from fuel combustion.  | A major contributor to global warming and climate change.                      |

**Table 5** Emission Factors Based on Machine Type and Pollutant Type

| Machine Type | Engine Type | Emission Factors ( $E_p$ g/kWh) |                 |      |        |      |                 |
|--------------|-------------|---------------------------------|-----------------|------|--------|------|-----------------|
|              |             | CO <sub>2</sub>                 | NO <sub>x</sub> | CO   | NM VOC | PM   | SO <sub>2</sub> |
| ME           | SSD         | 620.00                          | 17.00           | 1.40 | 0.632  | 1.39 | 10.50           |
| ME           | MSD         | 683.00                          | 13.00           | 1.10 | 0.527  | 1.39 | 11.50           |
| ME           | HSD         | 686.00                          | 12.70           | 1.00 | 0.527  | 1.39 | 11.31           |
| AE           | MSD         | 683.00                          | 13.00           | 1.10 | 0.421  | 1.39 | 12.30           |
| Boiler       | -           | 970.00                          | 2.10            | 0.20 | 0.105  | 0.57 | 16.50           |

**Table 6** Ship Main Activities and Emission Equations [16]

| Operation Modes | Matching                  | Emission Formula      |
|-----------------|---------------------------|-----------------------|
| Hoteling        | < 1kn                     | $E = E_b + E_c + E_p$ |
| Anchoring       | 1kn – 3kn                 | $E = E_b + E_c$       |
| Manoeuvring     | 3kn–8kn, < 20%MCR         | $E = E_a + E_b + E_c$ |
| Slow-steaming   | 8kn – 12kn, 20%MCR–65%MCR | $E = E_a + E_b$       |
| Cruising        | > 12kn, < 65kn            | $E = E_a + E_b$       |

Note that the values presented are energy-based emission factors (expressed in g/kWh). Most of the CO<sub>2</sub> emission factors are derived by multiplying the Specific Fuel Consumption (SFC) of each engine type with the corresponding fuel-based emission factors (in g CO<sub>2</sub>/g fuel). Similarly, SO<sub>2</sub> emission factors are determined based on the sulfur content of the fuel used.

These emission factor values are sourced from the Fourth IMO GHG Study 2020 and reflect the standard parameters adopted for various engine types, including slow-speed diesel (SSD), medium-speed diesel (MSD), high-speed diesel (HSD), auxiliary engines, and boilers.

## 2.5 Ship Activity Identification

When a ship is sailing, accelerating, or decelerating, its engines operate under varying conditions, including fuel consumption and engine performance, to generate the necessary power for movement. Consequently, emissions from ship engines differ depending on the ship's activity. Identifying various ship activities using AIS data is crucial for calculating ship exhaust emissions.

A ship is considered to be sailing if its speed exceeds 3 knots (1 knot = 1.852 km/h). This threshold distinguishes whether a ship is actively in motion or stationary. When sailing under typical operational conditions, a ship's instantaneous speed generally corresponds to approximately 85% of its engine's maximum capacity, as supported by operational data and modeling studies. [26]. AIS data shows that ships in motion generally exceed speeds of 12 knots. In contrast, manoeuvring speeds typically range between 3–8 knots, as vessels adjust their speed and direction when navigating into or out of ports, coastal waters, or areas with restricted visibility.

In the STEAM methodology, emission factors can vary according to fluctuations in the main engine load factor [17], [27].

Essentially, the Maximum Continuous Rated Engine Power (MCR) serves as the primary parameter representing the main engine load factor, as shown in Table 6.

## 2.6 Linear Regression Analysis to Determine Ship Power

The estimation of main engine power plays a crucial role in ship performance analysis and emissions assessment. However, due to data incompleteness in the current dataset, especially regarding power ratings, a direct regression modeling approach was not feasible. Therefore, this study adopted empirically validated regression equations developed in previous research to estimate main engine power based on ship dimensions.

Prior studies have shown a strong correlation between main engine power and the product of ship length and breadth, especially for cargo ships and tankers [14]. As a result, the present work utilizes existing polynomial regression models that relate engine power (kW) to the projected area of the hull (length × breadth, in m<sup>2</sup>). The equations (5) and (6) represent the power estimation models for cargo ships and tankers, respectively.

Cargo:

$$y = 7.52 \times 10^{-5} x^2 + 0.59x - 41.48 \quad (5)$$

Tanker:

$$y = 3.32 \times 10^{-5} x^2 + 0.27x - 57.20 \quad (6)$$

where  $x$  represents the product of the ship's length and width (m<sup>2</sup>) and  $y$  represents the ship's main engine power (kW).

This methodology provides a robust estimation technique for determining main engine power based on ship dimensions, which can be effectively utilized in ship performance assessments and emission monitoring systems [28].

The ratio of auxiliary engine power to main engine power varies depending on the type of ship. For example, car carriers have a ratio of 0.266, while bulk carriers, ocean tugs, and other unspecified ship types share a similar ratio of 0.222. Container ships exhibit a slightly lower ratio of 0.220, whereas cruise ships have a higher ratio of 0.278. General cargo ships demonstrate the lowest ratio at 0.191, while refrigerated ships have the highest ratio at 0.406. Roll-on ships show a ratio of 0.259, and tankers have a ratio of 0.211. These ratios are used to calculate the auxiliary engine power based on the ship's main engine power [16].

## 2.7 Design Speed

After determining the main engine power, it becomes possible to estimate the ship's design speed if it is not already known. This estimation relies on a regression model that correlates the design speed with the total engine power, particularly for tankers, container ships, and bulk carriers. For tankers and cargo vessels, the total main engine power can be derived using Equation 7 [28].

$$\begin{cases} CR = \alpha * DWT^{\beta} * V^{\gamma}, & \text{Mtanker} \\ CR = \alpha * TEU^{\beta} * V^{\gamma}, & \text{cargo} \end{cases} \quad (7)$$

Where MCR represents the total main engine power (measured in kilowatts) [kW], DWT denotes the deadweight tonnage of the tanker (in tons) [t], TEU indicates the number of containers, V refers to the design speed

(in knots), and  $\alpha$ ,  $\beta$ ,  $\gamma$  are the coefficients used in the regression model.

Using Equation 7, the design speed is determined inversely based on the calculated engine power. The resulting predictive formula for estimating the design speed of tankers and cargo vessels is provided in Equation 8.

$$\begin{cases} V_T = \sqrt[0.6]{MCR_T / 2.66 DWT^{0.6}}, & \text{tanker} \\ V_C = \sqrt[0.6]{MCR_T / 4.297 DWT^{0.6}}, & \text{cargo} \end{cases} \quad (8)$$

## 2.8 Methods

Ship Traffic Emission Model is a framework used to measure and analyze emissions produced by ships during sea operations. This model helps in understanding the environmental impact of shipping activities by calculating the number of emissions generated by various pollutants such as  $CO_2$ ,  $NO_x$ ,  $SO_x$ , and others [30].

The research method used in this study is inspired by the Ship Traffic Emission Model. However, there are important differences in the approach taken by the author. First, the author performs data preprocessing to clean raw data for easier processing. Then, to identify ship trajectories, the author uses a simple equation to determine sailing speed and time. Finally, the output of this research will be a website that displays processing results automatically in an integrated process. With this approach, the author hopes to provide a more efficient and accessible solution for stakeholders in understanding and controlling the environmental consequences of shipping practices.

The development flow of the ship emission monitoring system is illustrated in Figure 3, starting with the col-

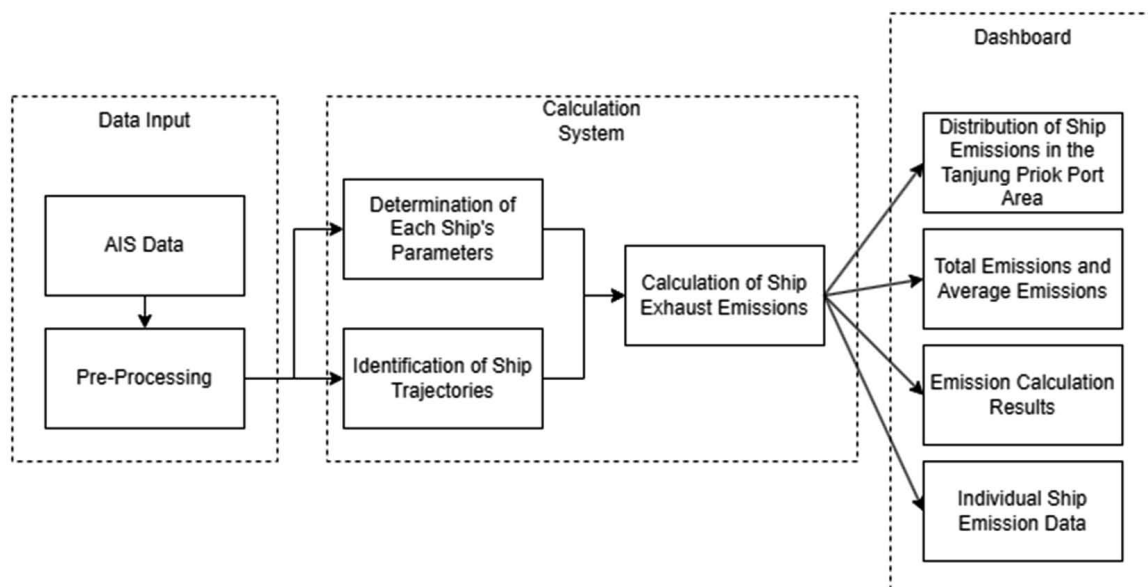


Figure 3 Research Flow Chart

lection of AIS data and a comprehensive literature review. Collected AIS data, which includes static and dynamic information about ships, undergoes preprocessing to ensure data quality and consistency. Static AIS data involves basic information about ships, such as Maritime Mobile Service Identity (MMSI), type, and dimensions. Meanwhile, dynamic AIS data includes real-time movement and activity information, such as coordinates, speed, and timestamps. This data is crucial for tracking ships and accurately assessing their emissions. Then, 15 AIS data samples are taken through the preprocessing process.

The next step is to determine parameters for each ship based on static AIS data. This involves updating AIS data according to MMSI to ensure accurate and up-to-date information. Regression analysis is then performed to estimate the power of the main and auxiliary engines as well as the design speed of the ship. These estimates are crucial for calculating ship emissions. Dynamic AIS data is used to identify ship trajectories. Each segment of the ship's journey is analyzed to calculate emissions using the STEAM model. This involves calculating sailing time and speed before estimating emissions for each segment and updating the ship emission database.

Finally, the processed data is visualized on an interactive web dashboard developed using Python, with front-end components built with HTML, CSS, and JavaScript. This dashboard provides monitoring and statistical visualization capabilities, enabling port authorities and stakeholders to make informed decisions to reduce the environmental impact of ship emissions. The entire system integrates data collection, processing, and visualization to provide a comprehensive tool for monitoring ship emissions at ports.

### 2.8.1 Preprocessing

Preprocessing AIS entails detecting, rectifying, or eliminating errors, inconsistencies, and anomalies within the dataset to guarantee that the data used for analysis or modeling is both reliable and accurate. This procedure, as illustrated in Figure 4, begins by loading raw data from CSV files using pandas, which is then organized into a structured format to allow for efficient manipulation and analysis. Key columns such as MMSI, name, IMO number, length, width, vessel type, latitude, longitude, and date time are retained, while unnecessary columns are removed to simplify the dataset. Duplicate entries are eliminated to maintain data integrity, and invalid coordinates are filtered to ensure spatial accuracy. Timestamp corrections and interpolations fill gaps for temporal reliability, while rows with invalid MMSI numbers or unrealistic ship dimensions are discarded. The cleaned data is then stored in a database for further use.

The database, designed to store AIS data for ship emission calculations, is implemented in MySQL. This database serves as a central repository that organizes AIS data, emissions, and other relevant data. The database structure, including tables, columns, data types, and relationships, is planned and created in detail using SQL commands. Data is entered manually or through automation scripts, and the MySQL database is integrated with the Django web framework for interactive data analysis and visualization. This process ensures a reliable and accurate dataset ready for the monitoring system.

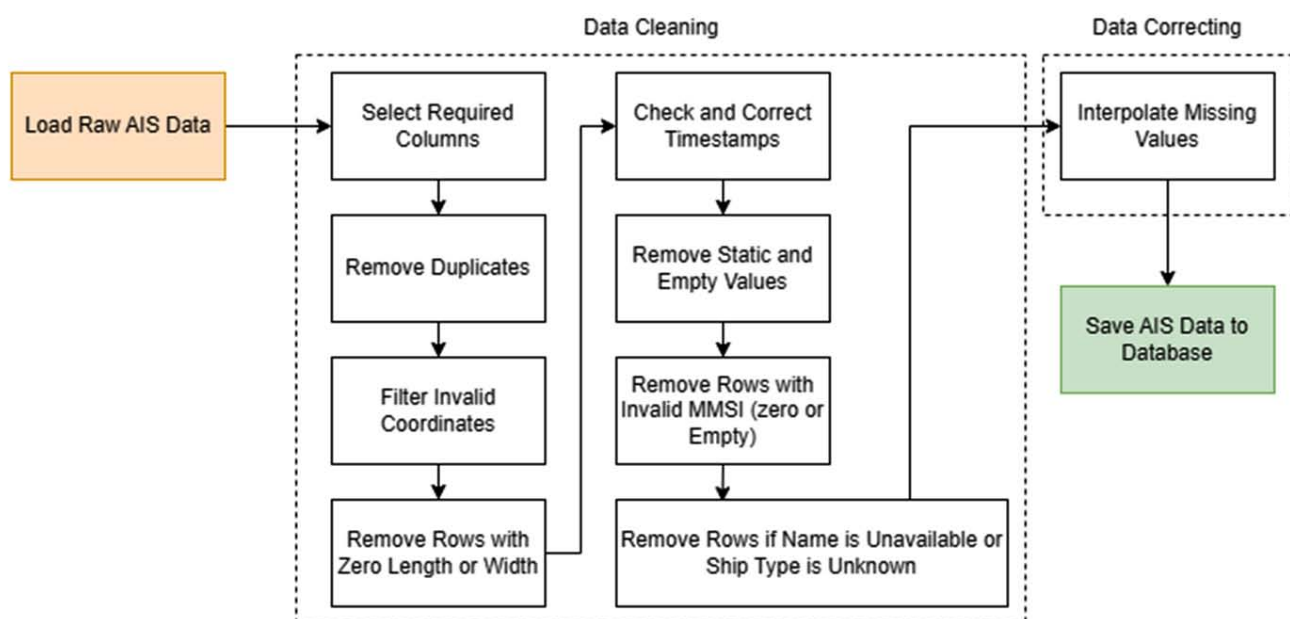


Figure 4 Preprocessing Flowchart

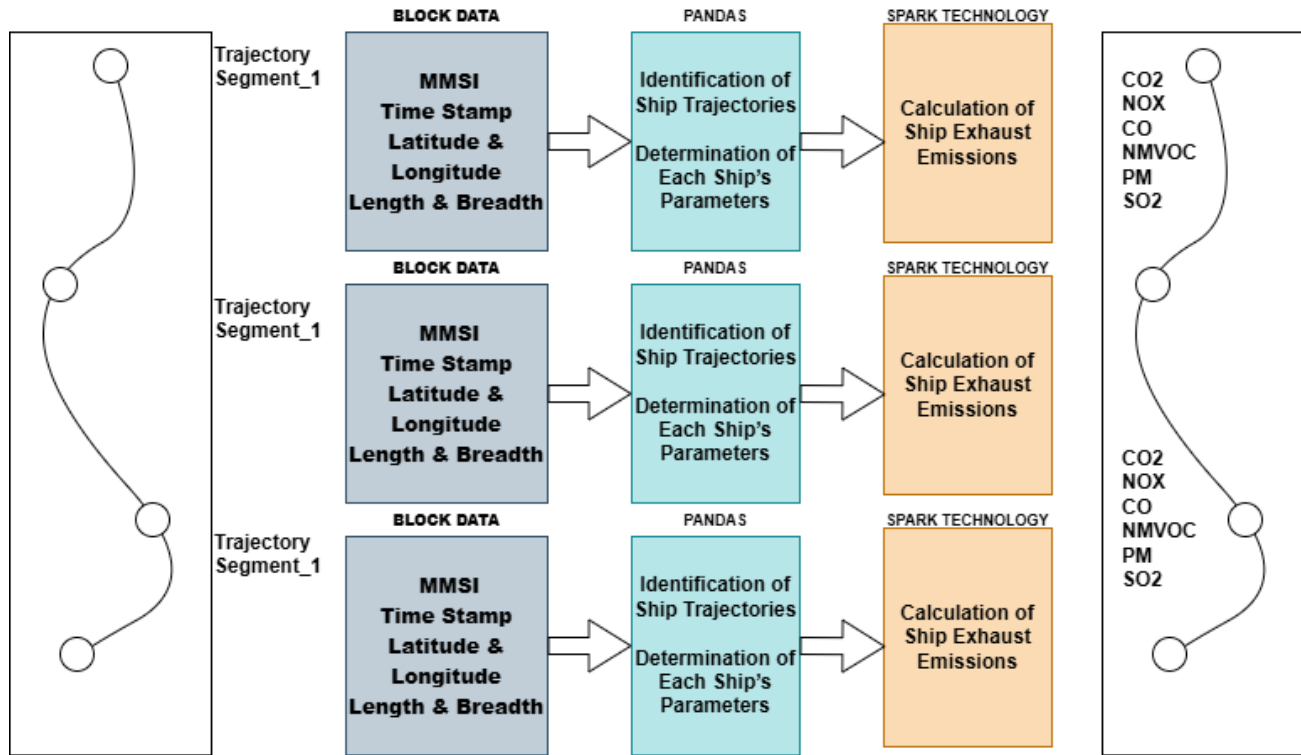


Figure 5 Distributed Emission Calculation Flow

### 2.8.2 Distributed Emission Calculation

Figure 5 illustrates the procedural framework for distributed emission calculations involves systematically assigning and processing computational tasks. The process begins, and data blocks are used to determine ship trajectories using Pandas. After trajectory segments are identified, ship parameters are calculated from these segments, using Pandas. Each segment of a ship's trajectory is subdivided into multiple data blocks, with each block serving as a fundamental unit for dynamic emission calculations. Once the data blocks are prepared, the Spark Engine allocates specific computational tasks to each block. These tasks utilize an advanced version of the STEAM model to estimate exhaust emissions for the corresponding trajectory segments. The tasks are executed in a First In, First Out (FIFO) sequence, ensuring systematic processing. Upon completion, the Spark Engine integrates the calculated emission results, which are promptly recorded in the database for further use.

After determining the selected MMSI for system development, AIS data is then sorted to produce data blocks that form trajectories for each ship. The calculation tasks are then assigned to calculate static and dynamic AIS data in a distributed manner. In this study, the author utilizes Pandas and Apache Spark to implement dynamic computational calculations. The calculations are carried out in sequence and efficiently process data blocks in batches within designated time intervals.

In the calculation process, key data elements such as emission factors and engine power ratios are critical for accurately estimating ship emissions using the STEAM model. Retrieving and processing this data manually would be highly time-consuming. To address this challenge, a big data storage solution, such as a MySQL database, is implemented to supply the essential information required for calculations efficiently. Prior to initiating the calculation process, this database ensures streamlined access to the necessary data, and these parameters will be arranged and stored in the database and connected to the calculations with the MySQL Connector so that the calculation program can easily access the required information.

The emission calculation process uses an enhanced version of the STEAM model proposed by [14] to estimate exhaust emissions from each ship. Equation 9 presents the formula for calculating ship exhaust emissions during sailing and mooring.

$$\begin{cases} E_i = P_m \times \left(\frac{\bar{v}_{ass}}{\bar{v}_{max}}\right)^3 \times T_m \times EF_{i,m} + P_a \times LF_a \times T_a \times EF_{i,a}, & \text{sailing} \\ E_i = P_a \times LF_a \times T_a \times EF_{i,a} + P_b \times T_b \times EF_{i,b}, & \text{mooring} \end{cases} \quad (9)$$

The subscript  $i$  indicates the specific type of pollutant, such as  $SO_x$ . The subscripts  $m$ ,  $a$ , and  $b$  correspond to the main engine, auxiliary engine, and ship boiler, respectively. The variable  $E$  represents the quantity of pollutant emissions, while  $P$  indicates the engine power.

Additionally, the variables  $P$  and  $T$  denote the power output and operational duration of the ship's engine. The parameters  $EF$  and  $LF$  signify the emission factor and load factor of the engine, respectively. Furthermore,  $V_{max}$  represents the design speed or maximum service speed, and  $V_{oss}$  indicates the ship's actual operating speed.

### 3 Results

#### 3.1 PreprocessingMA

The main data used for this research is the Big Data Automatic Identification System (AIS) provided by the Indonesian Maritime Security Agency (BAKAMLA RI). The collected AIS data focuses on the research object at Tanjung Priok Port.

Table 7 presents the specifications of AIS data received by the author, which include attributes such as MMSI, name, IMO, length, width, class, ship type, flag, COG, speed, latitude, longitude, destination, date time, heading, route, beam, draught, ETA, ship status, source, and flag.

The display of the ship trajectory validation program can be seen in Figure 6.

Figure 6 showing vessel movement and tracking accuracy in the Tanjung Priok Port area.

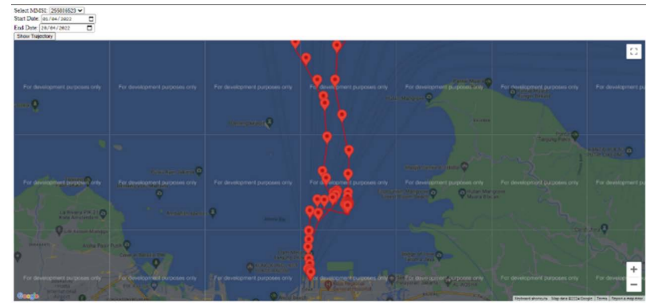


Figure 6 Displays of Ship Trajectory Validation Program

Based on this visualization, 15 ships from the obtained AIS data were identified using MMSI, as shown in Table 8.

Table 8 presents a list of tankers along with their key vessel attributes, including MMSI, name, IMO number, length, width, and vessel type. The data provides essential information for identifying and classifying tankers based on their dimensions and registration details. This dataset is useful for analyzing vessel characteristics, traffic patterns, and operational parameters within maritime logistics and port management.

Therefore, the sample AIS data records used total 16,432 records, as shown in Table 9.

Table 7 AIS Data RAW Specifications

| Number of AIS Records | Number of MMSI | Number of Ship Types | First Timestamp  | Last Timestamp   |
|-----------------------|----------------|----------------------|------------------|------------------|
| 1.048.576             | 1.031          | 25                   | 08/03/2022 17.00 | 09/06/2022 15.25 |

Table 8 Data on 15 Sample Ships

| MMSI      | Name            | IMO     | Length (Meter) | Width (Meter) | Vessel Type |
|-----------|-----------------|---------|----------------|---------------|-------------|
| 255806523 | APOLLO          | 9234628 | 26             | 167           | Tanker      |
| 256520000 | NEW RANGER      | 9328326 | 20             | 127           | Tanker      |
| 351169000 | ORALIA          | 9269609 | 18             | 118           | Tanker      |
| 354996000 | DIONNE          | 9814909 | 20             | 124           | Tanker      |
| 355332000 | DHEPOCH         | 9753648 | 22             | 120           | Tanker      |
| 370229000 | VALENTINE       | 9504023 | 21             | 134           | Tanker      |
| 374548000 | ASTREANA        | 9763629 | 14             | 97            | Tanker      |
| 441530000 | CT CONFIDENCE   | 9340427 | 24             | 145           | Tanker      |
| 525003041 | MT. ELISABET    | 9595668 | 10             | 75            | Tanker      |
| 525003175 | MT.KAKAP        | 9504401 | 18             | 108           | Tanker      |
| 525003489 | MT.LAPETTA      | 9004645 | 8              | 59            | Tanker      |
| 525004010 | PALU SIPAT      | 9106651 | 27             | 160           | Tanker      |
| 525004138 | TRANSCO AQUILA  | 9216042 | 14             | 93            | Tanker      |
| 525007033 | GAS MALUKU      | 9143154 | 20             | 100           | Tanker      |
| 525007196 | MT.FIGAR JAYA I | 9636230 | 57             | 9             | Tanker      |

**Table 9** AIS Data Note Sample Data (First five rows)

| MMSI      | Name   | IMO     | Width (meter) | Length (meter) | Vessel Type | Latitude | Longitude | Date Time           |
|-----------|--------|---------|---------------|----------------|-------------|----------|-----------|---------------------|
| 255806523 | APOLLO | 9234628 | 26            | 167            | Tanker      | -6.03596 | 106.9188  | 17/04/2022<br>06:37 |
| 255806523 | APOLLO | 9234628 | 26            | 167            | Tanker      | -6.03576 | 106.9181  | 17/04/2022<br>03:19 |
| 255806523 | APOLLO | 9234628 | 26            | 167            | Tanker      | -6.03714 | 106.9193  | 16/04/2022<br>22:10 |
| 255806523 | APOLLO | 9234628 | 26            | 167            | Tanker      | -6.03613 | 106.919   | 17/04/2022<br>07:16 |
| ...       | ...    | ...     | ...           | ...            | ...         | ...      | ...       | ...                 |

### 3.2 AIS Static Data Calculation Results

The calculation of AIS static data includes parameters such as main engine power, auxiliary engine power, and design speed data, which are computed using Python. To calculate the design speed, the ship's DWT data is required. The obtained DWT data is then entered into the database along with other supporting data. Table 10

shows the DWT data obtained according to the ships in the AIS sample data stored in the database.

The ship's DWT data is used to estimate the design speed, while the main and auxiliary engine power estimates use the ship's length and width data from the AIS records. The estimation results are presented in Table 11 and are then stored in the MySQL database.

**Table 10** Ship DWT data

| MMSI      | IMO     | Name             | Vessel Type | DWT (Tonnes) |
|-----------|---------|------------------|-------------|--------------|
| 255806523 | 9234628 | APOLLO           | Tanker      | 23998        |
| 256520000 | 9328326 | NEW RANGER       | Tanker      | 12950        |
| 351169000 | 9259609 | ORALIA           | Tanker      | 8715         |
| 354996000 | 9814909 | DIONNE           | Tanker      | 12384        |
| 355332000 | 9753648 | DH EPOCH         | Tanker      | 13204        |
| 370229000 | 9504023 | VALENTINE        | Tanker      | 14214        |
| 374548000 | 9763629 | ASTREANA         | Tanker      | 3654         |
| 441530000 | 9340427 | CT CONFIDENCE    | Tanker      | 19993        |
| 525003041 | 9595668 | MT. ELISABET     | Tanker      | 3255         |
| 525003175 | 9504401 | MT. KAKAP        | Tanker      | 6523         |
| 525003489 | 9004645 | MT. LAPETTA      | Tanker      | 730          |
| 525004010 | 9106651 | PALU SIPAT       | Tanker      | 17957        |
| 525004138 | 9216042 | TRANSCO AQUILA   | Tanker      | 3592         |
| 525007033 | 9143154 | GAS MALUKU       | Tanker      | 5761         |
| 525007196 | 9636230 | MT. FIGAR JAYA I | Tanker      | 1199         |

**Table 11** Estimation Results of Design Speed, Main Engine Power, and Auxiliary Ship

| MMSI      | Vessel_type | Main Engine Power (kW) | Auxiliary Engine Power (kW) | Speed_Design (Knots) |
|-----------|-------------|------------------------|-----------------------------|----------------------|
| 255806523 | Tanker      | 7488.724               | 1580.121                    | 23.39                |
| 256520000 | Tanker      | 2884.931               | 608.720                     | 8.84                 |
| 351169000 | Tanker      | 2128.457               | 449.104                     | 7.91                 |
| 354996000 | Tanker      | 2768.733               | 584.203                     | 8.63                 |
| 355332000 | Tanker      | 3083.907               | 650.704                     | 9.69                 |
| 370229000 | Tanker      | 3445.954               | 727.096                     | 10.83                |
| 374548000 | Tanker      | 1036.122               | 218.622                     | 5.69                 |
| 441530000 | Tanker      | 5017.453               | 1058.683                    | 14.40                |
| 525003041 | Tanker      | 446.450                | 94.201                      | 1.57                 |
| 525003175 | Tanker      | 1836.753               | 387.555                     | 8.27                 |
| 525003489 | Tanker      | 258.604                | 54.566                      | 2.64                 |
| 525004010 | Tanker      | 7419.517               | 1565.518                    | 30.78                |
| 525004138 | Tanker      | 971.548                | 204.997                     | 5.20                 |
| 525007033 | Tanker      | 1925.200               | 406.217                     | 10.13                |
| 525007196 | Tanker      | 299.811                | 63.260                      | 2.19                 |

### 3.3 AIS Dynamic Data Calculation Results

Sailing speed is calculated by dividing the distance travelled between sequential AIS data points by the time difference. This calculation is essential for categorizing ship activities and understanding their operational modes. Table 12 shows the results of the sailing speed calculations.

Sailing time is calculated by determining the time difference between sequential AIS data points for each ship. The total sailing time is calculated by summing these differences, providing a comprehensive measure of the ship's activity duration.

The results of the sailing time calculations are shown in Table 13.

**Table 12** Total Ship Sailing Time (First Three Rows)

| MMSI      | Speed (knots) | Date Time        |
|-----------|---------------|------------------|
| 255806523 | 10.84703643   | 16/04/2022 05:50 |
| 255806523 | 10.06962199   | 16/04/2022 06:01 |
| 255806523 | 10.89496867   | 16/04/2022 06:14 |
| ...       | ...           | ...              |

**Table 13** Ship Sailing Speed (first three lines)

| MMSI      | Duration | Start Timestamp  | End Timestamp    |
|-----------|----------|------------------|------------------|
| 255806523 | 0.18     | 16/04/2022 05:50 | 16/04/2022 06:01 |
| 255806523 | 0.22     | 16/04/2022 06:01 | 16/04/2022 06:14 |
| 255806523 | 0.20     | 16/04/2022 06:14 | 16/04/2022 06:26 |
| ...       | ...      | ...              | ...              |

### 3.4 Ship Emission Calculation Results

Once all the necessary variables are complete, the ship emission calculation process can be carried out. In this experiment, the time period from April 1, 2022, to April 20, 2022, was used as shown in Table 14. The data required for the calculations is taken directly from the MySQL database.

Table 14 presents the analysis of ship emission data collected over a 20-day period from April 1, 2022, to April 20, 2022, for 15 ships revealed significant variability in various emission parameters, providing insight of the ecological effects of maritime activities. The emission data analysis revealed important insights into the distribution and characteristics of various pollutants. It is important to note that data showing a value of 0 re-

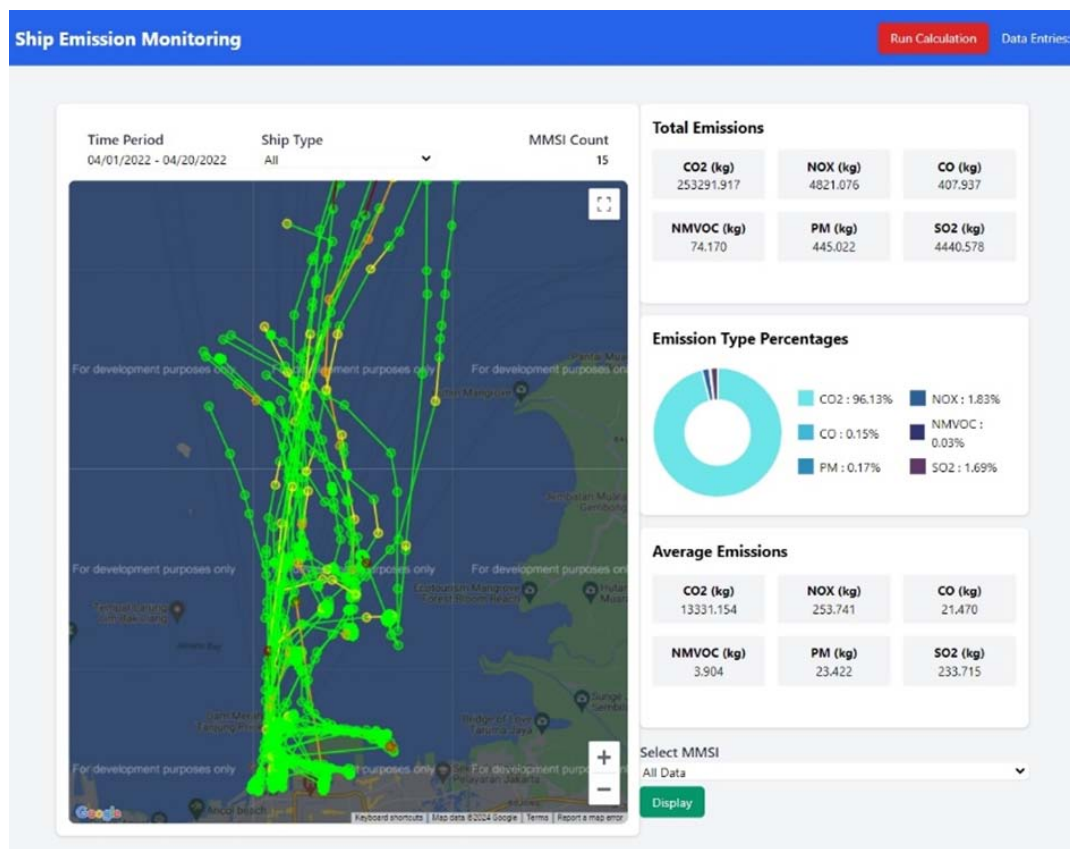
flects situations where the calculated data duration is 0, resulting in the emission calculation being 0 as well. This can occur when ships are docked in port or undergoing loading and unloading processes.

This dataset consists of total recorded emissions dominated by CO<sub>2</sub>, accounting for 96.12% of total emissions, amounting to (253,291.927 kg). This is followed by NO<sub>x</sub> at 1.83% (4,821.076 kg), SO<sub>2</sub> at 1.69% (4,440.578 kg), PM at 0.17% (445.022 kg), CO at 0.15% (407.937 kg), and NMVOC at 0.03% (74.170 kg). The percentage of these emission types highlights the dominance of CO<sub>2</sub> in contributing to total emissions. In terms of average emissions per pollutant type recorded, CO<sub>2</sub> again leads with an average emission of 13,331.154 kg. NO<sub>x</sub> follows with an average of 253.741 kg, SO<sub>2</sub> with 233.715 kg, PM with 23.422 kg, CO with 21.470 kg, and NMVOC with 3.904 kg.

**Table 14** Deduction of ship emissions calculation results (with time period 04/01/2022 – 04/20/2022)

| MMSI      | CO <sub>2</sub> (Kg) | NO <sub>x</sub> (Kg) | CO (Kg) | NMVOC (Kg) | PM (Kg) | SO <sub>2</sub> (Kg) |
|-----------|----------------------|----------------------|---------|------------|---------|----------------------|
| 255806523 | 955.743              | 18.191               | 1.539   | 0.280      | 1.679   | 16.113               |
| 255806523 | 1129.514             | 21.499               | 1.819   | 0.331      | 1.985   | 19.043               |
| ...       | ...                  | ...                  | ...     | ...        | ...     | ...                  |
| 256520000 | 334.716              | 6.371                | 0.539   | 0.098      | 0.588   | 5.643                |
| 256520000 | 267.773              | 5.097                | 0.431   | 0.078      | 0.470   | 4.515                |
| ...       | ...                  | ...                  | ...     | ...        | ...     | ...                  |
| 351169000 | 296.338              | 5.640                | 0.477   | 0.087      | 0.521   | 4.996                |
| 351169000 | 98.779               | 1.880                | 0.159   | 0.029      | 0.174   | 1.665                |
| ...       | ...                  | ...                  | ...     | ...        | ...     | ...                  |
| 354996000 | 674.592              | 12.840               | 1.086   | 0.198      | 1.185   | 11.373               |
| 354996000 | 14385.481            | 7.337                | 0.621   | 0.113      | 0.677   | 6.499                |
| ...       | ...                  | ...                  | ...     | ...        | ...     | ...                  |
| 355332000 | 429.361              | 8.172                | 0.692   | 0.126      | 0.754   | 7.239                |
| 355332000 | 26.734               | 0.509                | 0.043   | 0.008      | 0.047   | 0.481                |
| ...       | ...                  | ...                  | ...     | ...        | ...     | ...                  |
| 370229000 | 239.884              | 4.566                | 0.386   | 0.070      | 0.421   | 4.044                |
| 370229000 | 159.923              | 3.044                | 0.258   | 0.047      | 0.281   | 2.696                |
| ...       | ...                  | ...                  | ...     | ...        | ...     | ...                  |
| 374548000 | 120.213              | 2.288                | 0.194   | 0.035      | 0.211   | 2.027                |
| 374548000 | 12.021               | 0.229                | 0.019   | 0.004      | 0.021   | 0.203                |
| ...       | ...                  | ...                  | ...     | ...        | ...     | ...                  |
| 441530000 | 349.281              | 6.648                | 0.563   | 0.102      | 0.614   | 5.889                |
| 441530000 | 174.641              | 3.324                | 0.281   | 0.051      | 0.307   | 2.944                |
| ...       | ...                  | ...                  | ...     | ...        | ...     | ...                  |
| 525003041 | 4.838                | 0.092                | 0.008   | 0.001      | 0.008   | 0.087                |
| 525003041 | 4.838                | 0.092                | 0.008   | 0.001      | 0.008   | 0.087                |
| ...       | ...                  | ...                  | ...     | ...        | ...     | ...                  |
| 525003175 | 277.035              | 5.273                | 0.446   | 0.081      | 0.487   | 4.671                |
| 525003175 | 213.104              | 4.056                | 0.343   | 0.062      | 0.374   | 3.593                |
| ...       | ...                  | ...                  | ...     | ...        | ...     | ...                  |
| 525003489 | 2.242                | 0.043                | 0.004   | 0.001      | 0.004   | 0.040                |
| 525003489 | 2.242                | 0.043                | 0.004   | 0.001      | 0.004   | 0.040                |
| ...       | ...                  | ...                  | ...     | ...        | ...     | ...                  |
| 525004010 | 1205.159             | 22.939               | 1.941   | 0.353      | 2.117   | 20.318               |
| 525004010 | 258.248              | 4.915                | 0.416   | 0.076      | 0.454   | 4.354                |
| ...       | ...                  | ...                  | ...     | ...        | ...     | ...                  |
| 525004138 | 8.422                | 0.160                | 0.014   | 0.002      | 0.015   | 0.152                |
| 525004138 | 8.422                | 0.160                | 0.014   | 0.002      | 0.015   | 0.152                |
| ...       | ...                  | ...                  | ...     | ...        | ...     | ...                  |
| 525007033 | 178.693              | 3.401                | 0.288   | 0.052      | 0.314   | 3.013                |
| 525007033 | 178.693              | 3.401                | 0.288   | 0.052      | 0.314   | 3.013                |
| ...       | ...                  | ...                  | ...     | ...        | ...     | ...                  |
| 525007196 | 34.785               | 0.662                | 0.056   | 0.010      | 0.061   | 0.586                |
| 525007196 | 34.785               | 0.662                | 0.056   | 0.010      | 0.061   | 0.586                |
| ...       | ...                  | ...                  | ...     | ...        | ...     | ...                  |

### 3.5 Monitoring Dashboard



#### Emission Data

| MMSI      | Start Timestamp     | End Timestamp       | Vessel Type | CO <sub>2</sub> (kg) | NO <sub>x</sub> (kg) | CO (kg)               | NMVOC (kg)           |
|-----------|---------------------|---------------------|-------------|----------------------|----------------------|-----------------------|----------------------|
| 525003489 | 2022-04-01 00:00:00 | 2022-04-01 00:12:00 | Tanker      | 2.241781518779489    | 0.04266934076739876  | 0.0036104826803183576 | 0.000656451396421519 |
| 525004138 | 2022-04-01 00:04:00 | 2022-04-01 00:16:00 | Tanker      | 8.422125395084716    | 0.1603039972710122   | 0.013564184384470263  | 0.002466215342630956 |
| 525003041 | 2022-04-01 00:11:00 | 2022-04-01 00:26:00 | Tanker      | 4.837716375468139    | 0.09207952105576252  | 0.007791344089333752  | 0.001416608016242500 |

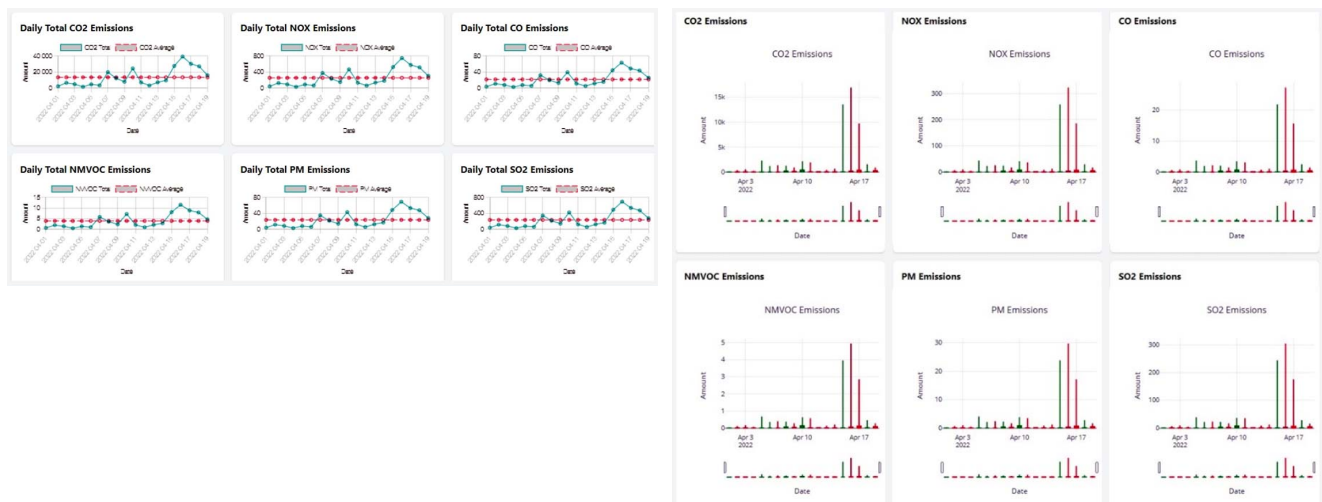


Figure 7 Monitoring Dashboard User Interface

The user interface (UI) is designed to be intuitive and user-friendly to facilitate access and interpretation of complex emission data, as shown in Figure 7. User feedback indicates that the interface effectively conveys data, with users appreciating the interactive map and real-time data updates. The ability to visualize emissions spatially and temporally provides stakeholders with a clear understanding of emission patterns and their implications. Front-end development plays a crucial role in enhancing the accessibility and usability of the emission monitoring system, supporting informed decision-making and policy development.

The back-end system also performs well, efficiently handling multiple data requests and ensuring timely updates to the front-end. This design is intended to scale with increasing data volumes to ensure that the system can accommodate future AIS data and emission calculations. The integration of Django with the MySQL database enables seamless data interaction and processing, meeting the requirements of the ship emission monitoring system. The back-end development provides a solid foundation for the overall system's functionality and performance, ensuring that data is processed and delivered accurately and efficiently.

## 4 Discussion

The proposed big data-based framework for a ship emission monitoring system is adaptable for implementation in other ports where high maritime traffic significantly contributes to air pollution. As long as ships within a port area are required to transmit AIS data, this data can be processed and utilized as a source for emission monitoring. Expanding this system would enable real-time emission tracking, allowing port authorities to develop localized control strategies and ensure compliance with IMO's MARPOL Annex VI [31] and national regulations. Integrating this system across multiple ports would facilitate data-sharing and coordinated policy-making, enhancing the port's efforts to reduce greenhouse gas emissions in maritime operations. Although the system has been tested using historical AIS data, it has not yet been validated against real-world emission measurement data. This validation process is identified as a key objective for future system development. Successful implementation requires digital infrastructure readiness, operational adaptability, and regulatory alignment, ensuring a seamless transition to a unified national ship emission monitoring network.

## 5 Conclusions

This research aims to develop a web-based ship emission monitoring system that utilizes AIS data and various related calculations to provide comprehensive

information on ship pollutant emissions through a system supported by a structured MySQL database that stores emission and other operational ship data. The system is integrated with the Django framework to retrieve, process, and display data through an interactive and user-friendly web interface that can be used by decision-makers, primarily at Tanjung Priok Port, in efforts to control ship emissions in the port area.

To enhance system automation, future work will involve validating the estimated emissions against actual onboard emission measurements to improve the system's accuracy and reliability. Implementing a DWT estimation method or alternatively providing access to classification society data or port data would be beneficial. Developing faster calculation methods is also necessary to process larger datasets. Furthermore, developing more detailed calculation methods tailored to the Tanjung Priok Port area is needed.

**Funding:** This work is supported by the "Hibah Publikasi Terindeks Internasional (PUTI) Pascasarjana 2024-2025" funded by DRPM Universitas Indonesia under contract No. NKB-115/UN2.RST/HKP.05.00/2024.

**Acknowledgments:** We would like to thank the following individuals and organizations for their invaluable contributions to this research. The Indonesian Maritime Security Agency (BAKAMLA RI) for providing the AIS data used in this study.

**Author Contributions:** Andi Wibisono: Conceptualization, Methodology, Data Collection, Data Curation, Formal Analysis, Investigation, Writing – Original Draft, Writing – Review & Editing, Validation, Verification / Mathematical Harmonization, Final Approval; Achmad Riadi: Supervision, Methodology, Writing – Review & Editing, Funding Acquisition, Final Approval; Muhammad Aqil Taqiyyuddin: Data Collection, Writing – Review & Editing; Muhammad Arif Budiyanto: Formal Analysis, Writing – Review & Editing; Dimas Angga Fakhri Muzhoffar: Investigation, Data Curation.

## References

- [1] F. Alver, B. A. Saraç, and Ü. Alver Şahin, "Estimating of shipping emissions in the Samsun Port from 2010 to 2015," *Atmos Pollut Res*, vol. 9, no. 5, pp. 822–828, Sep. 2018, doi: 10.1016/j.apr.2018.02.003.
- [2] International Maritime Organization. (2020). Fourth IMO GHG Study 2020: Full report. IMO. <https://www.imo.org/en/OurWork/Environment/Pages/Fourth-IMO-Greenhouse-Gas-Study-2020.aspx>.
- [3] Y. Wang, E. Zio, X. Wei, D. Zhang, and B. Wu, "A resilience perspective on water transport systems: The case of Eastern Star," *International Journal of Disaster Risk Reduction*, vol. 33, pp. 343–354, Feb. 2019, doi: 10.1016/j.ijdr.2018.10.019.

- [4] V. Eyring, H. W. Köhler, A. Lauer, and B. Lemper, "Emissions from international shipping: 2. Impact of future technologies on scenarios until 2050," *Journal of Geophysical Research D: Atmospheres*, vol. 110, no. 17, pp. 183–200, Sep. 2005, doi: 10.1029/2004JD005620.
- [5] N. R. Ammar and I. S. Seddiek, "Eco-environmental analysis of ship emission control methods: Case study RO-RO cargo vessel," *Ocean Engineering*, vol. 137, pp. 166–173, Jan. 2017, doi: 10.1016/j.oceaneng.2017.03.052.
- [6] S. Vutukuru and D. Dabdub, "Modeling the effects of ship emissions on coastal air quality: A case study of southern California," *Atmos Environ*, vol. 42, no. 16, pp. 3751–3764, May 2008, doi: 10.1016/j.atmosenv.2007.12.073.
- [7] D. A. Schwarzkopf, R. Petrik, V. Matthias, M. Quante, E. Majamäki, and J. P. Jalkanen, "A ship emission modeling system with scenario capabilities," *Atmos Environ X*, vol. 12, p. 100132, Dec. 2021, doi: 10.1016/j.aeaoa.2021.100132.
- [8] H. Liu et al., "Health and climate impacts of ocean-going vessels in East Asia," *Nat Clim Chang*, vol. 6, no. 11, pp. 1037–1041, Nov. 2016, doi: 10.1038/nclimate3083.
- [9] I. Mamoudou, F. Zhang, Q. Chen, P. Wang, and Y. Chen, "Characteristics of PM<sub>2.5</sub> from ship emissions and their impacts on the ambient air: A case study in Yangshan Harbor, Shanghai," *Science of the Total Environment*, vol. 640, pp. 207–216, Nov. 2018, doi: 10.1016/j.scitotenv.2018.05.261.
- [10] H. Lindstad, B. E. Asbjørnslett, and A. H. Strømman, "Reductions in greenhouse gas emissions and cost by shipping at lower speeds," *Energy Policy*, vol. 39, no. 6, pp. 3456–3464, Jun. 2011, doi: 10.1016/j.enpol.2011.03.044.
- [11] S. K. W. Ng et al., "Policy change driven by an AIS-assisted marine emission inventory in Hong Kong and the Pearl River Delta," *Atmos Environ*, vol. 76, pp. 102–112, Sep. 2013, doi: 10.1016/j.atmosenv.2012.07.070.
- [12] J. P. Jalkanen, A. Brink, J. Kalli, H. Pettersson, J. Kukkonen, and T. Stipa, "A modelling system for the exhaust emissions of marine traffic and its application in the Baltic Sea area," *Atmos Chem Phys*, vol. 9, no. 23, pp. 9209–9223, 2009, doi: 10.5194/acp-9-9209-2009.
- [13] L. Fink et al., "Potential impact of shipping on air pollution in the Mediterranean region - A multimodel evaluation: Comparison of photooxidants NO<sub>2</sub> and O<sub>3</sub>," *Atmos Chem Phys*, vol. 23, no. 3, pp. 1825–1862, 2023, doi: 10.5194/acp-23-1825-2023.
- [14] L. Huang, Y. Wen, Y. Zhang, C. Zhou, F. Zhang, and T. Yang, "Dynamic calculation of ship exhaust emissions based on real-time AIS data," *Transp Res D Transp Environ*, vol. 80, Mar. 2020, doi: 10.1016/j.trd.2020.102277.
- [15] Z. Wan, S. Ji, Y. Liu, Q. Zhang, J. Chen, and Q. Wang, "Shipping emission inventories in China's Bohai Bay, Yangtze River Delta, and Pearl River Delta in 2018," *Mar Pollut Bull*, vol. 151, Feb. 2020, doi: 10.1016/j.marpolbul.2019.110882.
- [16] J. Weng, K. Shi, X. Gan, G. Li, and Z. Huang, "Ship emission estimation with high spatial-temporal resolution in the Yangtze River estuary using AIS data," *J Clean Prod*, vol. 248, p. 119297, Mar. 2020, doi: 10.1016/j.jclepro.2019.119297.
- [17] L. Huang, Y. Wen, X. Geng, C. Zhou, C. Xiao, and F. Zhang, "Estimation and spatio-temporal analysis of ship exhaust emission in a port area," *Ocean Engineering*, vol. 140, pp. 401–411, Aug. 2017, doi: 10.1016/j.oceaneng.2017.06.015.
- [18] Y. Shu et al., "Evaluation of ship emission intensity and the inaccuracy of exhaust emission estimation model," *Ocean Engineering*, vol. 287, p. 115723, Nov. 2023, doi: 10.1016/j.oceaneng.2023.115723.
- [19] T. Topic, A. J. Murphy, K. Pazouki, and R. Norman, "Assessment of ship emissions in coastal waters using spatial projections of ship tracks, ship voyage and engine specification data," *Clean Eng Technol*, vol. 2, p. 100089, Jun. 2021, doi: 10.1016/j.clet.2021.100089.
- [20] S. Song, "Ship emissions inventory, social cost and eco-efficiency in Shanghai Yangshan port," *Atmos Environ*, vol. 82, pp. 288–297, Jan. 2014, doi: 10.1016/j.atmosenv.2013.10.006.
- [21] L. Starcrest Consulting Group, "PORT OF LONG BEACH AIR EMISSIONS INVENTORY," 2010. Accessed: Sep. 28, 2024. [Online]. Available: [https://longbeach.granicus.com/DocumentViewer.php?file=longbeach\\_7dcdcb6a1e0f29166ab58b91dec9c5b9.pdf&utm\\_source=chatgpt.com](https://longbeach.granicus.com/DocumentViewer.php?file=longbeach_7dcdcb6a1e0f29166ab58b91dec9c5b9.pdf&utm_source=chatgpt.com).
- [22] D. Chen et al., "Estimating ship emissions based on AIS data for port of Tianjin, China," *Atmos Environ*, vol. 145, pp. 10–18, Nov. 2016, doi: 10.1016/j.atmosenv.2016.08.086.
- [23] J. Moreno-Gutiérrez, V. Durán-Grados, Z. Uriondo, and J. Ángel Llamas, "Emission-factor uncertainties in maritime transport in the Strait of Gibraltar, Spain," Aug. 2012, doi: 10.5194/amtd-5-5953-2012.
- [24] Y. Zhang et al., "Shipping emissions and their impacts on air quality in China," *Science of The Total Environment*, vol. 581–582, pp. 186–198, Mar. 2017, doi: 10.1016/j.scitotenv.2016.12.098.
- [25] M. Zhou, W. Jiang, W. Gao, X. Gao, M. Ma, and X. Ma, "Anthropogenic emission inventory of multiple air pollutants and their spatiotemporal variations in 2017 for the Shandong Province, China," *Environmental Pollution*, vol. 288, p. 117666, Nov. 2021, doi: 10.1016/j.envpol.2021.117666.
- [26] OCIMF, "Compliance with EEXI Regulation," vol. 1, 2024, [Online]. Available: [www.ocimf.org](http://www.ocimf.org)
- [27] H. X. H. L. Z. Z. Y. S. Y. Q. W. C. S. X. C. H. Zhou, "Main engine power estimation method for the inland ship based on big data," *Journal of Dalian Maritime University*, vol. 45, pp. 44–49, 2019, doi: 10.16411/j.cnki.
- [28] T. Cepowski, "Regression Formulas for The Estimation of Engine Total Power for Tankers, Container Ships and Bulk Carriers on The Basis of Cargo Capacity and Design Speed," *Polish Maritime Research*, vol. 26, no. 1, pp. 82–94, Mar. 2019, doi: 10.2478/pomr-2019-0010.
- [30] S. Deng and Z. Mi, "A review on carbon emissions of global shipping," *Marine Development*, vol. 1, no. 1, p. 4, Nov. 2023, doi: 10.1007/s44312-023-00001-2.
- [31] "International Maritime Organization." Accessed: Apr. 17, 2024. [Online]. Available: International Convention for the Prevention of Pollution from Ships (MARPOL).